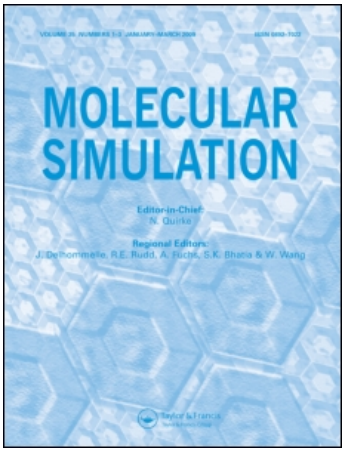

Molecular Simulation
Publication details, including instructions for authors and subscription information:
http://www.informaworld.com/smpp/title~content=t713644482

Molecular Dynamics Study on Protein and it's Water Structure at High Pressure

Chong Chul Chai[a]; Mu Shik Jhon[a]
[a] Department of Chemistry and Center for Molecular Science, Korea Advanced Institute of Science and Technology, Taejon, Korea

To cite this Article Chai, Chong Chul and Jhon, Mu Shik(2000) 'Molecular Dynamics Study on Protein and it's Water Structure at High Pressure', Molecular Simulation, 23: 4, 257 — 274
To link to this Article: DOI: 10.1080/08927020008025372
URL: http://dx.doi.org/10.1080/08927020008025372

Molecular Simulation, 2000, Vol. 23, pp. 257–274
Reprints available directly from the publisher
Photocopying permitted by license only

MOLECULAR DYNAMICS STUDY ON PROTEIN AND IT'S WATER STRUCTURE AT HIGH PRESSURE

CHONG CHUL CHAI and MU SHIK JHON*

Department of Chemistry and Center for Molecular Science,
Korea Advanced Institute of Science and Technology, 373-1 Kusung-dong
Yusung-gu, Taejon 305-701, Korea

(Received August 1999; Accepted August 1999)

We have performed NPT molecular dynamics simulations (Langevin Piston Method) on two types of solvated proteins–"denaturation-unfavorable" protein (insulin) and "denaturation-favorable protein" (ribonuclease A) at high pressure (from 1 bar up to 20 kbar). The method is based on the extended system formalism introduced by Andersen, where the deterministic equations of motion for the piston degree of freedom are replaced by Langevin equation. We report the structural changes of proteins (ribonuclease A and insulin) and water molecules through radius of gyration, solvent accessible surface area, hydrogen bond pattern, and the topology of water clusters connected by the hydrogen bonded circular network. The solvent accessibility of ribonuclease A is mainly decreased by hydrophilic residues rather than hydrophobic residues under high pressure. From the results of hydrogen bond analysis, we have found that α-helix is more stable than β-sheet under high pressure. In addition, from the analysis of the water cluster, we have observed that for ribonuclease A, 5-membered ring structure is more favorable than 6-membered ring at higher pressure. However, for insulin, the ratio of 5 to 6-ring is constant over the pressure ranges for which we have performed MD simulation. This indicates that the water structure around insulin does not change under high pressure.

Keywords: Simulation; molecular dynamics; high pressure; water structure; hydrogen bond; surface area

1. INTRODUCTION

Recent pressure-induced denaturation studies of protein have offered some clues about the problem of protein folding. Since the works of Brandts [1], Weber [2] and Zipp [3], numerous experiments have been done: Raman [4],

*Corresponding author. e-mail: jwater@sorak.kaist.ac.kr

NMR [5], Fluorescence [6], X-ray scattering [7] and FT-IR combined with hydrogen-deuterium exchange experiments [8–13]. Silvar and Weber [14] summarized the pressure effects on the stability of single chain proteins as follows:

- Proteins undergo reversible conformational transitions that result in spectral changes at hydrostatic pressures of 5 kbar or more.
- These spectral changes occur within a small pressure interval of 0.5–1.5 kbar. This indicates that the appearance of a protein conformation is different from the native one with a smaller volume. The decrease in volume of the solvated protein is on the order of 0.2–0.5%.
- Fluorescence data indicate that in the "high pressure" conformation the tryptophan residues are in contact with a medium that has the polarity of water.
- Hydrodynamic data show that the protein retains its globular form.

Generally, the pressure denaturation of globular protein is reversible in the range of 4–5 kbar. Beyond this range, precipitates or gels can form. The denaturated protein structure is not always like a random-coil, but may retain significant structures of the native proteins. The volume change during pressure denaturation is small compared with that during thermal denaturation.

Protein stability is determined by many factors, such as, its structural characteristics, intra-molecular interaction and environmental interaction. Among these factors, the hydrogen bond, electrostatic interaction, and hydrophobic effect have been treated as main subjects [15].

However, the studies of pressure and temperature effects have not given detailed information on the atomic level. Molecular simulations [16–23] compensated for this drawback.

Molecular dynamics simulations can be used to study the conformational freedom of proteins in solvent at atmospheric pressure and the behavior of proteins and water under high pressure conditions. A comparison of molecular dynamics simulations at high and low pressure can give microscopic insights into pressure induced denaturation; the results are consistent with the results obtained by experimental methods. The previous NPT molecular dynamics simulation at high pressure [20–22] have been performed using the Berendsen algorithm [29]. However, this algorithm may have some limitations (not describing the exact NPT ensemble, but the NPH ensemble). So, in high pressure MD, we have adopted the Langevin Piston method [30], which is modified from Nose-Hoover algorithm and describes the NPT ensemble more exactly.

The systems on which we have performed the MD simulation are ribonuclease A and insulin. Ribonuclease A, a small monomeric enzyme, consists of 124 amino acids with an N-terminal α-helix and two shorter helices packed against 3 central twisted anti-parallel β-sheets. Ribonuclease A from bovine pancreas has been the subject of many protein folding and stability studies over the years with lysozyme, chymotrypsinogen, *etc.* Insulin is a small (51 amino acid) hormone important for regulating the cellular uptake of glucose over longer time periods and necessary for normal cell growth and proliferation. Insulin consists of two chains – an A chain of 21 residues and a B chain of 30 residues – which are covalently joined by two disulfide links (and another disulfide bond is formed in the A chain itself). In its secondary structure, it has a total of 3 α-helices. (two α-helices in the A chain and one α-helix in the B chain). In the FT-IR experiments [9], insulin was not denatured at high pressure (above 13.2 kbar), while ribonuclease A was denatured at 8.5 kbar through a reversible process.

The purpose of this work is to compare the protein conformation, including the solvent structure at high pressure, with that in a normal pressure and to show the important factors affecting pressure-induced denaturation. We do this by comparing with ribonuclease A and insulin, which are known as "denaturation favorable" and "denaturation unfavorable" proteins at high pressure, respectively.

We performed a long simulation (total 1 ns) under different pressure conditions (from 1 bar to 20 kbar) in order to detect the events that are involved in the earlier stages of the unfolding of the protein under high pressure. To analyze the process, we have investigated the radius of gyration, the volume fluctuation, the solvent accessible surface area and the water structure.

2. METHODS

The starting structures of ribonuclease A (3RN3) and insulin (9INS) were obtained from the Brookhaven Protein Data Bank (Upton, NY). The empirical energy function used here, is the CHARMM polar hydrogen model in which polar hydrogen atoms are treated explicitly and non-polar hydrogens (CH_3, CH_2, CH) are incorporated into the heavy atoms to which they are bonded [24, 25]. A TIPS3P [26] model was used for describing water. Water bonds and angles were constrained by SHAKE [27]. We placed the proteins at the center of rectangular boxes with a dimension of $X = 55.87776$ Å, $Y = 49.66912$ Å, $Z = 40.35616$ Å for ribonuclease A and $X = 46.5648$ Å,

$Y = 37.25184$ Å, $Z = 37.25184$ Å for insulin. Filling the boxes with water molecules resulted in the addition of 2976 water molecules for the ribonuclease A and 1769 for the insulin with resultant system density of 0.999188 g/cm^3 and 0.96736 g/cm^3, respectively.

The conditions of MD simulations were as the follows: the time step employed was 1 fs; the bond lengths were constrained to equilibrium values using the SHAKE algorithm [27]; the nonbonded interactions were spherically truncated at 8 Å (CTOFNB). The electrostatic interactions were shifted to zero at 8 Å (CTONB) and van der Waals interactions were switched off from 7 to 8 Å. The nonbonded list was generated with an 9 Å cutoff (CUTNB). For the nonbonded list update, the heuristic test was performed every time energy was called for and a list update was done if necessary. The conventional periodic boundary conditions were applied during the simulations.

Only the solvent molecules were minimized by the steepest descent algorithm, fixing the protein, followed by full minimization of 1000 steps for the protein and solvent molecules. The whole minimization was also performed by the steepest descent and adopted basis newton rapson method. The system was warmed up to 298 K under 1 bar for 6 ps and equilibrated for 40 ps.

The production runs were continued for 160 ps at 1 bar. And then, the pressure was increased 1 bar up to 20 kbar (1 bar, 5, 10, 15, 20 kbar). During these steps, a molecular dynamics simulation was performed for 200 ps (including equilibration of 40 ps) at each pressure, and we used the last 120 ps per each stage in order to analyze the results.

The equations of motion were integrated using the leapfrog algorithm which is considered to be the most stable in molecular dynamics, especially in NPT simulation [28]. The temperature and pressure of the systems were controlled by the Langevin piston method [30]. For the pressure and temperature mass, we used the 225 atomic mass unit (amu) and 100 Kcal ps^2, respectively. Also, for collision frequency (γ), 20 ps^{-1} was used. At this condition, the unnatural oscillations in the virial associated with the piston mass were eliminated. The same simulation scheme and conditions were adopted for both insulin and ribonuclease A systems.

The accessible surface area of the protein was calculated using Richard's method [31]. A 1.4-Å probe radius was used for all calculations. Protein volumes were calculated according to the connolly method [32] using a probe radii of 1.4 and 0 Å (*i.e.*, the volume enclosed by the van der Waals surface). For the analysis of hydrogen bonds, the following criterion was used: the proton donor to heavy-atom acceptor distance must be less than

2.6 Å and the hydrogen-bond angle (A — X ··· X) must be greater than 135 degrees. For the analysis of the ring structure, the hydrogen-bond criteria were the same as above. Detailed explanations for selecting ring structure were given in the article of Yu *et al.* [33]. However, we used the geometry criteria were used instead of the hydrogen-bond energy criteria for computational convenience.

3. RESULTS AND DISCUSSION

3.1. Radius of Gyration and Volume Fluctuation

In Figure 1, the radius of gyration (RGYR) of the ribonuclease A shrinks step-wisely from an initial value of 14.75 Å at 1 bar to ~ 14 Å at 10 kbar and converges to 14 Å after the initial big change. In contrast, the RGYR of insulin gradually decreases from 10.0 to 9.5 Å.

Figure 2 shows the time evolution of the protein volume over 600 ps simulations. The volume of ribonuclease A greatly decreases at 1 bar–10 kbar, is stable at 10 kbar–15 kbar, and decreases by a large amount at 15 kbar–20 kbar. However, the volume of the insulin decreases slowly over all the simulations. The patterns of volume fluctuation are consistent with the results of RGYR. These results from RGYR and the volume fluctuation of the proteins are consistent with the experiment [9], in which the ribonuclease A is denaturated at 8.5 kbar, but the insulin remains in its native form above 13.2 kbar. This indicates that ribonuclease A is more sensitive to external pressure than insulin.

3.2. Solvent Accessible Surface Area (SASA)

Figure 3 shows, the trajectories of the solvent accessible surface area (SASA) of ribonuclease A for polar residues including charged groups, non-polar residues, and the whole protein. The SASA of the polar groups of ribonuclease A decreases remarkably by ~ 200 Å^2 in 10 kbar and converges to 20 kbar, as shown in Figure 3(C). In the non-polar groups (Ala, Val, Leu, Ile and Phe), which are known to determine the protein compressibility, there are only small fluctuations as shown in Figure 3(B). Comparing Figure 3(A) and Figure 3(C) reveal that the main contribution to the SASA decrease of ribonuclease A is from the polar groups rather than the non-polar residues. From the decreased total solvent accessibility of ribonuclease A, we can deduce that the hydrophobic residues in protein surfaces are relatively more exposed than charged or polar residues. This was expected

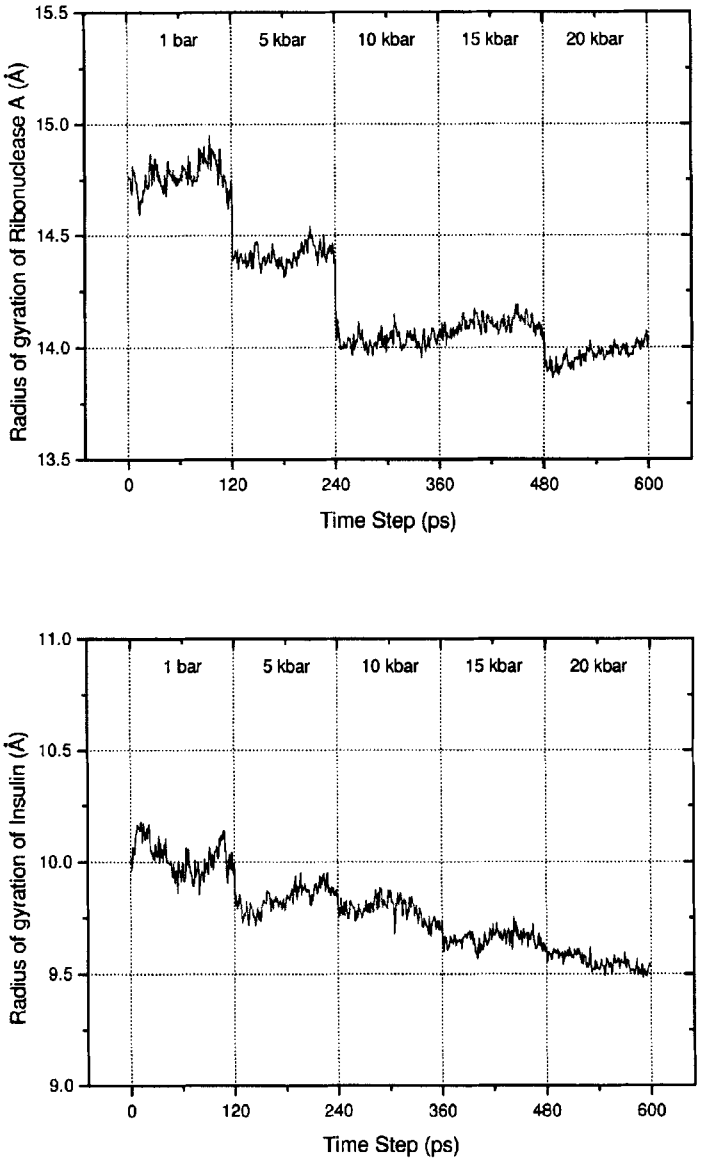

FIGURE 1 Time trajectory of the radius of gyration in 600 ps of molecular dynamics simulation; ribonuclease A (upper) and insulin (lower).

from previous pressure simulation [20–22]. That is, the polar residues penetrate into the core of the protein, and the partial accessibility of a polar residues are relatively increased by the penetrated polar groups.

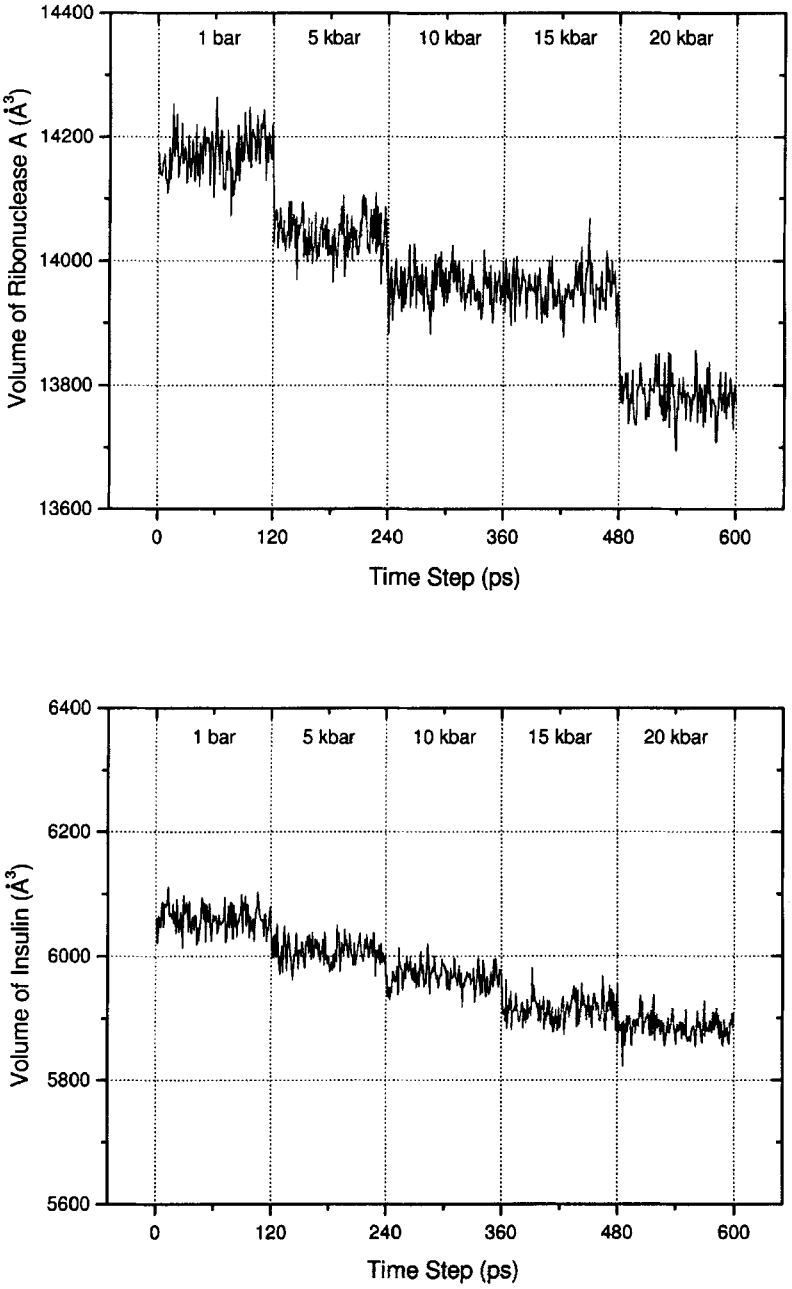

FIGURE 2 Time trajectory of the volume of ribonuclease A (upper) and insulin (lower) in 600 ps of molecular dynamics simulation.

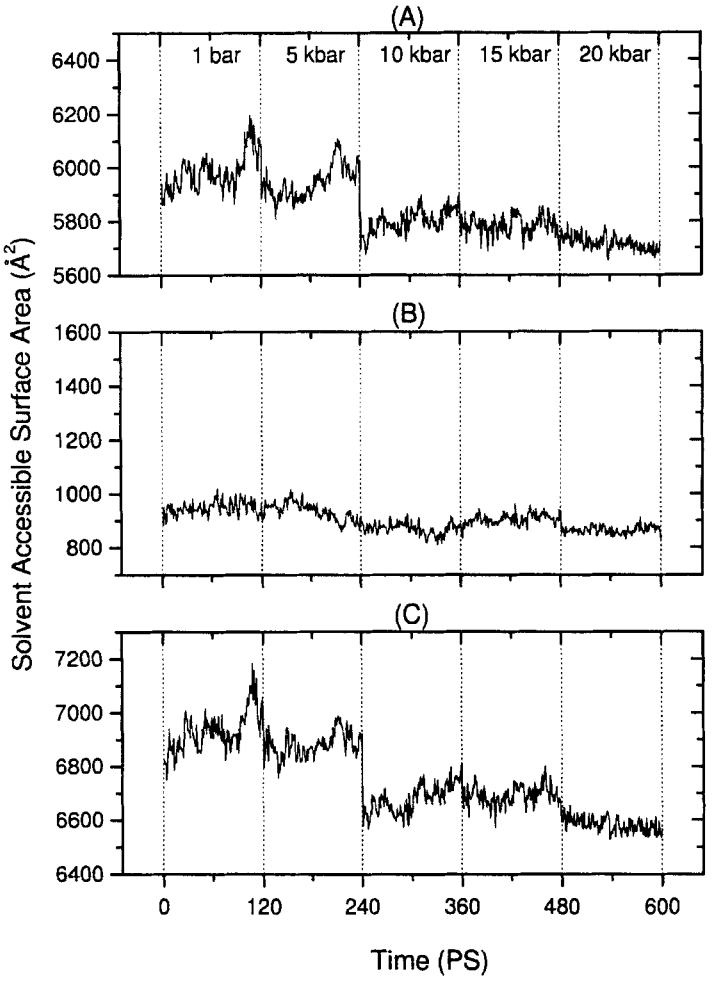

FIGURE 3 Solvent Accessible Surface Area of polar (A) groups, non-polar (B) groups and whole protein (C) of Ribonuclease A during the simulation.

Figure 4 shows the trajectory of the solvent accessible surface area of insulin. The changes as much as ribonuclease A are not shown in the SASA of polar groups and a whole insulin. Apparently, the change of accessibility of the polar groups does not influence the exposure of hydrophobic residues as much as ribonuclease A. This is probably because the strong hydrophobic core comprised of three helix does not permit polar the residues to penetrate into the insulin core.

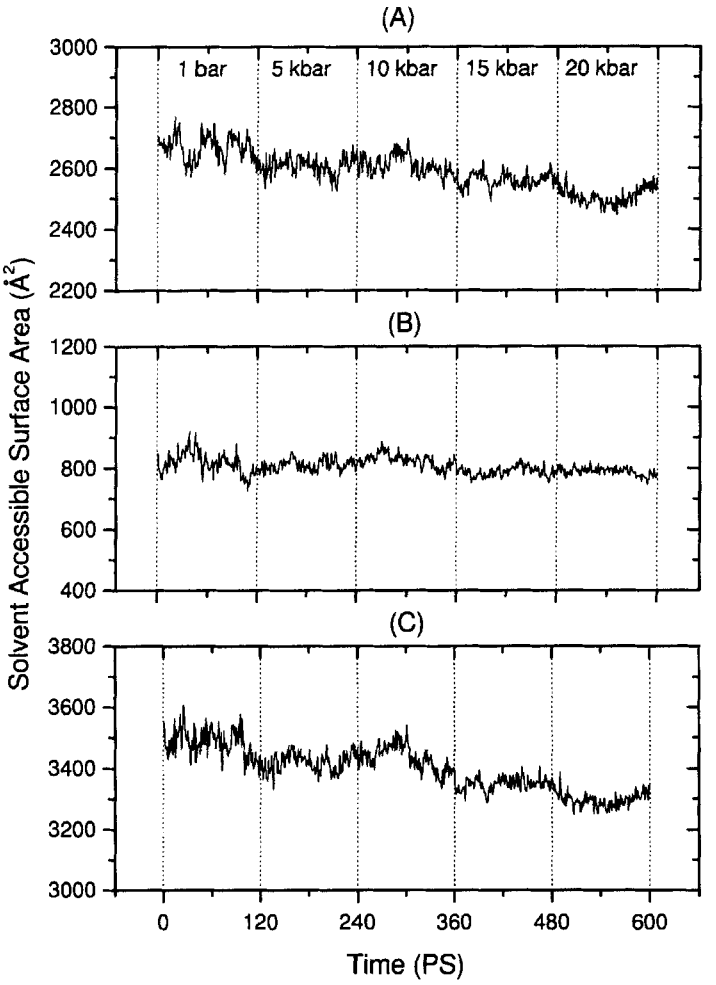

FIGURE 4 Solvent Accessible Surface Area of polar (A) groups, non-polar (B) groups and whole protein (C) of insulin during the simulation.

Figure 5 and Figure 6 show the accessibility of the secondary structure of each protein. In the case of ribonuclease A, the change of β-sheet starts at 5 kbar, whereas that of α-helix is initiated at 10 kbar. The turn structures exhibit only a slight change in SASA. This may be due to the difference of the compressibility of secondary structure. Therefore, β-sheet structures close to the protein surface are earlier influenced than α-helix by pressure. In the case of insulin, the SASA of the turn structure increases gradually, and that of α-helix has no specific change.

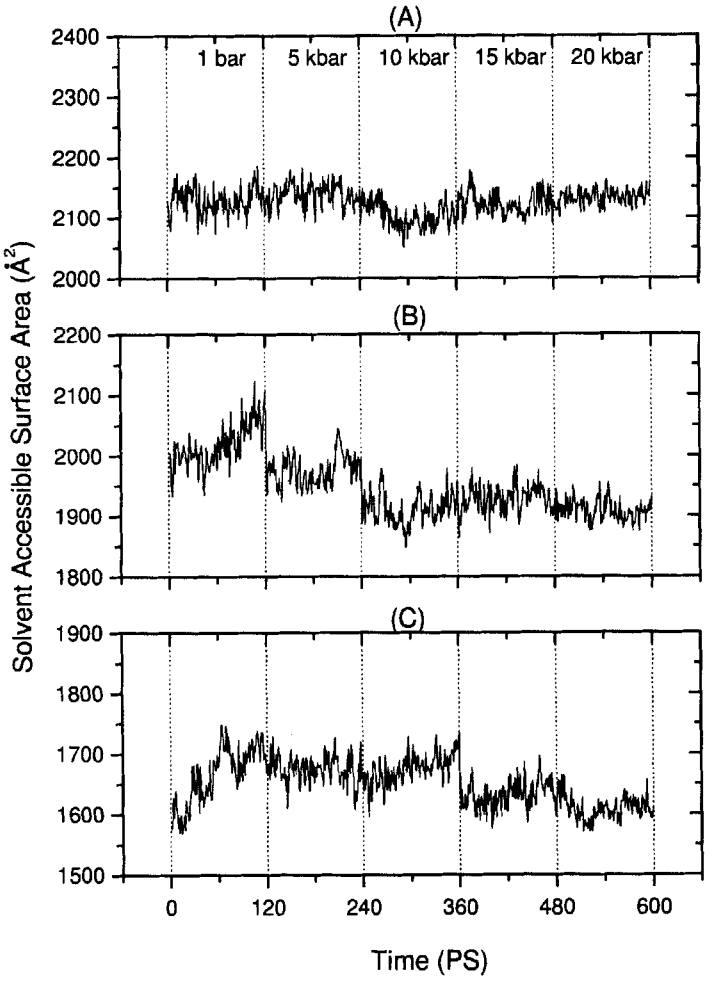

FIGURE 5 Solvent Accessible Surface Area of turn(A), β-sheet(B) and α-helix(C) of ribonuclease A during the simulation.

3.3. Hydrogen Bonds

It is important to examine the time evolution of inter-molecular or intramolecular hydrogen bonds because this water environment plays an important role in protein unfolding. The relative strength of the inter- and intramolecular interactions is reflected by the balance of protein–protein, protein–water, and water–water hydrogen bonds. For a system in balance, for instance the native state of a protein in solution, this ratio, as well as the total number of hydrogen bonds, should be constant. A higher pressure strengthens the interactions where water is involved, relative to that in the proteins.

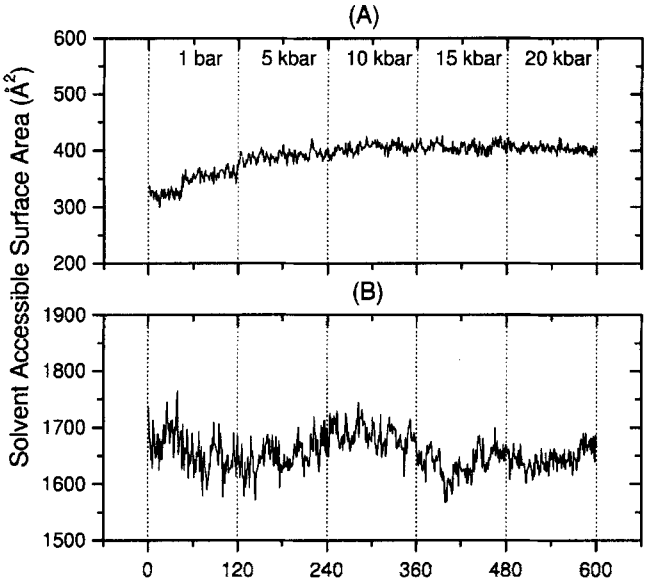

FIGURE 6 Solvent Accessible Surface Area of turn(A) and α-helix(B) of Insulin during the simulation.

As expected, water–water hydrogen bonds and water–protein hydrogen bonds increases as pressure increases, whereas the number of intra-molecular hydrogen bonds decreases in ribonuclease A. (Tab. I). This indicates that the increase of intra-molecular hydrogen bonds (water–water and water–protein) compensates for the cleavage of intra-molecular HB mainly in protein backbone. In addition, the cleavage amount of β-strand corresponds to that of a whole ribonuclease A. However the number of hydrogen bonds of α-helix are not disrupted all over the simulations. It is compatible with the results from solvent accessible surface area.

In Table II, which shows the hydrogen bonds list of insulin, we did not detected any kinds of intra-molecular cleavages. And the hydrogen bond number of α-helix of insulin increases slightly. This indicates that the α-helix is more stable than β-sheet under high pressure.

3.4. Distribution of Ring Structure

Water molecules connected by hydrogen bonds form various kinds of small clusters. Intensive interest has been focused on the hydrogen-bonded circular network. The distribution of the ring of hydrogen bonded molecules is greatly affected by conditions such as pressure and temperature.

Table III and Table IV show the occurrence of each ring and the ratio of pentamer to hexamer (R5/6), which are known to be important in biological

TABLE I Number of hydrogen bonds in ribonuclease A

	Ribonuclease A				
Hydrogen bonds	1 *bar*	5 *kbar*	10 *kbar*	15 *kbar*	20 *kbar*
α-helix	23.47 (2.43)[a]	23.73 (2.17)	23.51 (1.97)	23.20 (1.85)	23.11 (1.83)
β-sheet	25.69 (2.76)	22.16 (2.44)	21.18 (2.99)	20.58 (2.91)	20.16 (2.75)
Intra HB	95.09 (5.08)	90.11 (4.56)	91.44 (4.70)	91.66 (4.26)	91.24 (4.79)
Protein $\cdots$ water HB	102.62 (5.18)	108.34 (4.30)	110.44 (4.93)	111.26 (4.67)	112.38 (4.79)
Water $\cdots$ water HB	4718.86 (25.89)	4764.88 (26.82)	4894.57 (26.40)	4898.09 (26.47)	4936.23 (24.44)

[a] Standard Deviation.

TABLE II Number of hydrogen bonds in insulin

Hydrogen bonds	*Insulin*				
	1 bar	*5 kbar*	*10 kbar*	*15 kbar*	*20 kbar*
α-helix	13.81 (1.68)[a]	15.32 (1.77)	14.26 (1.50)	15.10 (1.47)	15.03 (1.47)
Intra HB	32.39 (2.91)	32.62 (2.86)	32.54 (2.80)	32.56 (2.81)	33.42 (2.69)
Protein···water HB	42.67 (3.03)	44.52 (2.96)	45.82 (3.13)	44.50 (3.34)	45.66 (2.74)
Water···water HB	2658.63 (20.70)	2705.86 (21.48)	2733.21 (20.49)	2752.08 (21.18)	2769.06 (20.84)

[a] Standard Deviation.

TABLE III The water ring structure around ribonuclease A

	Ribonuclease A				
Occurrence	1 *bar*	5 *kbar*	10 *kbar*	15 *kbar*	20 *kbar*
3-ring	5.329[a] (68.088)[b]	6.061 (80.638)	6.754 (92.956)	7.100 (98.013)	7.627 (106.412)
4-ring	15.811 (202.031)	16.535 (219.994)	17.394 (239.406)	18.433 (254.463)	19.221 (268.169)
5-ring	32.812 (419.269)	33.739 (448.900)	37.850 (520.950)	38.183 (527.094)	38.493 (537.050)
6-ring	46.048 (588.388)	43.666 (580.981)	38.001 (523.025)	36.284 (500.887)	34.660 (483.575)
R5/6 ratio[c]	0.713	0.773	0.996	1.052	1.111

[a] the percentage (%) of each ring to the total ring structure.
[b] the averaged number of each ring structure.
[c] the ratio of 5-ring to 6-ring.

TABLE IV The water ring structure around insulin

	Insulin				
Occurrence	1 *bar*	5 *kbar*	10 *kbar*	15 *kbar*	20 *kbar*
3-ring	5.342[a] (34.150)[b]	6.081 (42.725)	6.663 (48.475)	7.027 (52.292)	7.419 (56.392)
4-ring	16.514 (105.575)	17.002 (119.450)	17.941 (130.533)	18.893 (140.600)	20.057 (152.450)
5-ring	33.319 (213.017)	32.363 (227.375)	31.896 (232.067)	31.406 (233.717)	30.765 (233.842)
6-ring	44.826 (286.583)	44.553 (313.017)	43.501 (316.500)	42.674 (317.567)	41.759 (317.400)
R5/6 ratio[c]	0.743	0.726	0.733	0.736	0.737

[a] the percentage (%) of each ring to the total ring structure.
[b] the averaged number of each ring structure.
[c] the ratio of 5-ring to 6-ring.

systems. In the ribonuclease A, the 6-ring structure (46.05%) is more dominant than the pentamer structure (32.81%) at a normal pressure, but the percentage of the 6-ring decreases by $\sim 12\%$, whereas that of the 5-ring increases by $\sim 6\%$ under induced high pressure. After all, the ratio of 5 to 6-ring is reversed after 15 kbar pressure (0.713 at 1 bar $\rightarrow$ 1.052 at 15 kbar). This may be because the water structure around ribonuclease A changes under high pressure, and the prevalence of the 5-ring structure makes some effects on pressure-induced protein denaturation.

Table IV shows that for insulin, the R5/6 ratio is 0.743 at a normal pressure and slightly decreases to 0.737 up to 20 kbar. This indicates that insulin may favor 6-ring ordering at higher pressure and 1 bar, and have a different solvent environment from ribonuclease A.

4. CONCLUSION

In this article, we reported the results of molecular dynamics simulations for pressure denaturation of ribonuclease A and insulin under high pressure. The high pressure MD simulations are performed by the modified Nose-Hoover algorithm (Langevin Piston method) and not the Berendsen method, for the first time.

Ribonuclease A, a denaturation favorable protein at high pressure, has the following properties. (1) The volume of the protein is considerably shrunk. (2) The hydrophobic residues in protein surface are more exposed relative to other hydrophilic (charged or polar) residues. This originates from penetration of the hydrophilic residues to the core of the protein. (3) Hydrogen bonds especially of β-sheet structure are cleaved and the number of intra-molecular hydrogen bonds (water–water and protein–water) increases to keep the system in balance. This partial cleavage of the β-sheet in ribonuclease A may show up at earlier stages of the protein unfolding. Whereas, α-helix structures of both proteins are remained as native form. (4) The water structure around ribonuclease A, in which the 6-ring structure is dominant under normal pressure condition, changes to a 5-ring dominant structure relatively at higher pressure. This small change in the water environment influences the conformation of the protein. However, the water structure around insulin has no change under high pressure and this result is consistent with previous experiment [9].

We have presented molecular dynamics simulation of two kinds of proteins, which have different denaturation properties under high pressure.

This work allows us to describe at microscopic levels the events involved in high pressure induced conformational transitions.

Acknowledgement

This work was supported in part by the Korea Research Center for Theoretical Physics and Chemistry.

References

[1] Brandts, J. F., Oliveira, R. J. and Westort, C. (1970). "Thermodynamics of protein denaturation. Effect of pressure on the denaturation of Ribonuclease A", *Biochemistry*, **9**, 1083–1047.
[2] Weber, G. and Drickamer, H. G. (1983). "The effect of high pressure upon proteins and other biomolecules", *Q. Rev. Biophys.*, **16**, 89–112.
[3] Zipp, A. and Kauzmann, W. (1973). "Pressure denaturation of metmyoglobin", *Biochemistry*, **12**, 4217–4228.
[4] Kato, M. and Taniguchi, Y. (1994). "Raman study on the conformation equilibrium of 1,3-dichloropropane in the liquid phase", *J. Phys. Chem.*, **98**, 2688–2693.
[5] Jonas, J., Ballard, L. and Nash, D. (1998). "High-resolution, high pressure NMR studies of proteins", *Biophys. J.*, **75**, 445–452.
[6] Royer, C. A., Hinck, A. P., Loh, S. N. and Markley, J. L. (1993). "Effects of Amino Acid substitutions on the pressure denaturation of staphylococcal nuclease as monitored by Fluorescence and NMR spectroscopy", *Biochemistry*, **32**, 5222–5232.
[7] Panick, G., Malessa, R., Winter, R., Rapp, G., Frye, K. J. and Royer, C. A. (1998). "Structural Characterization of the pressure-denatured state and unfolding/refolding kinetics of staphylococcal nuclease by synchrotron small-angle X-ray scattering and FT-IR spectroscopy", *J. Mol. Biol.*, **275**, 389–402.
[8] Takeda, N., Kato, M. and Taniguchi, Y. (1995). "Pressure- and thermal-induced reversible changes in the secondary structure of ribonuclease A studied by FT-IR spectroscopy", *Biochemistry*, **34**, 5980–5987.
[9] Taniguchi, Y. and Takeda, N. (1992). "Pressure-induced secondary structure of proteins studied by FT-IR spectroscopy", *High Pressure and Biotechnology*, Balny, C., Hayashi, R., Heremans, K. and Masson, P., Eds., Colloque INSERM/Jhon Libbey Eurotext, **224**, 115–122.
[10] Akasaka, K., Tezuka, T. and Yamada, H. (1997). "Pressure-induced changes in the folded structure of lysozyme", *J. Mol. Biol.*, **271**, 671–678.
[11] Goossens, K., Smeller, L., Frank, J. and Heremans, K. (1996). "Pressure-tuning the conformation of BPTI studied by FT-IR spectroscopy", *Eur. J. Biochem.*, **236**, 254–262.
[12] Wong, P. T. T. and Heremans, K. (1988). "Pressure effects on protein secondary structure and hydrogen deuterium exchange in chymotrypsinogen: FT-IR spectroscopic study", *Biochim. Biopys. Acta.*, **956**, 1–9.
[13] Li, H., Yamada, H. and Akasaka, K. (1988). "Effect of pressure on individual hydrogen bonds in proteins. basic PTI", *Biochemistry*, **37**, 1167–1173.
[14] Silva, J. L. and Weber, G. (1993). "Pressure stability of proteins", *Annu. Rev. Phys. Chem.*, **44**, 89–113.
[15] Dill, K. A. (1990). "Dominant Forces in Protein Folding", *Biochemistry*, **29**, 7133–7155.
[16] Daggett, V. and Levitt, M. (1992). "A model of the molten globule state from molecular dynamics simulations", *Proc. Natl. Acad. Sci.*, **89**, 5142–5146.

[17] Mark, A. E. and van Gunsteren, W. F. (1992). "Simulation of the thermal denaturation of hen egg white lysozyme: trapping the molten globule state", *Biochemistry*, **31**, 7745–7748.
[18] Brunne, R. M. and van Gunsteren, W. F. (1993). "Dynamical properties of bovine pancreatic trypsin inhibitor from a molecular dynamics simulation at 5000 atm", *FEBS*, **323**, 215–217.
[19] Norberg, J. and Nilsson, L. (1994). "High-pressure molecular dynamics of a nucleic acid fragment", *Chem. Phys. Lett.*, **224**, 219–224.
[20] Kitchen, D. B., Reed, L. H. and Levy, R. M. (1992). "Molecular dynamics simulation of solvated protein at high pressure", *Biochemistry*, **31**, 10083–10093.
[21] Yu, J. Y., Kang, N. S. and Jhon, M. S. (1995). "Pressure and temperature dependence study of the denaturation of ribonuclease a solutions", *Mol. Sim.*, **15**, 265–272.
[22] Wroblowski, B., Diaz, J. F., Heremans, K. and Engelborghs, Y. (1996). "Molecular mechanisms of pressure induced conformational changes in BPTI", *Proteins Struct. Funct. Genet.*, **25**, 446–455.
[23] Hünenberger, P. H., Mark, A. E. and van Gunsteren, W. F. (1995). "Computational approaches to study protein unfolding: Hen egg white lysozyme as a case study", *Proteins Struct. Funct. Genet.*, **21**, 196–213.
[24] Brooks, B. R., Bruccoleri, R. E., States, D. J., Swaminathan, S. and Karplus, M. (1983). "CHARMM: A program for macromolecular energy minimization and dynamics calculations.", *J. Comput. Chem.*, **4**, 187–217.
[25] Neria, E., Fischer, S. and Karplus, M. (1996). "Simulation of activation free energy in molecular systems", *J. Chem. Phys.*, **105**, 1902–1921.
[26] Jorgensen, W. L., Chandrasekhar, J., Madura, J. D., Impey, R. W. and Klein, M. L. (1983). "Comparison of simple potential functions for simulating liquid water.", *J. Chem. Phys.*, **79**, 926–935.
[27] van Gunsteren, W. F. and Berendsen, H. J. C. (1977). "Algorithms for macromolecular dynamics and constraint dynamics", *Mol. Phys.*, **34**, 1311–1327.
[28] Toxvaerd, S. (1993). "Molecular dynamics at constant temperature and pressure", *Phys. Rev. E*, **47**, 343–350.
[29] Berendsen, H. J. C., Postma, J. P. M., van Gunsteren, W. F., Dinola, A. and Haak, J. R. (1984). "Molecular dynamics with coupling to an external bath", *J. Chem. Phys.*, **81**, 3684–3690.
[30] Feller, S. E., Zhang, Y. and Pastor, R. W. (1995). "Constant pressure molecular dynamics simulation: The Langevin piston method", *J. Chem. Phys.*, **103**, 4613–4621.
[31] Richards, F. M. (1977). "Areas, volumes, packing, and protein structure", *Annu. Rev. Biophys. Bioeng.*, **6**, 151–176.
[32] Connolly, M. L. (1985). "Computation of molecular volume", *J. Am. Chem. Soc.*, **107**, 1118–1124.
[33] Yu, J. Y., Shin, J. K. and Jhon, M. S. (1994). "The structure of water in human ras oncogene proteins", *Int. J. Quan. Chem.*, **51**, 241.